

Manuscript Number: JMB-D-10-01288R1

Title: MEMBRANE INSERTION AND TOPOLOGY OF THE TRANSLOCATING CHAIN-ASSOCIATING MEMBRANE PROTEIN (TRAM)

Article Type: Full Length Article

Section/Category: Membrane structure and transport

Keywords: membrane protein; topology; TRAM; photocrosslinking; translocon

Corresponding Author: Associate Professor Ismael Mingarro, PhD

Corresponding Author's Institution: Universitat de Valencia

First Author: Silvia Tamborero

Order of Authors: Silvia Tamborero; Marçal Vilar, PhD; Luis Martínez-Gil, PhD; Arthur E Johnson, PhD; Ismael Mingarro, PhD

Abstract: The translocating chain-associating membrane protein (TRAM) is a glycoprotein involved in the translocation of secreted proteins into the ER lumen, and in the insertion of integral membrane proteins into the lipid bilayer. As a major step toward elucidating the structure of the functional endoplasmic reticulum (ER) translocation/insertion machinery, we have characterized the membrane integration mechanism and the transmembrane (TM) topology of TRAM using two approaches: photocross-linking and truncated C-terminal reporter tag fusions. Our data indicate that TRAM is recognized by the signal recognition particle (SRP) and translocon components, and suggest a membrane topology with eight TM segments, including several poorly hydrophobic segments. Furthermore, we studied the membrane insertion capacity of these poorly hydrophobic segments into the ER membrane by themselves. Finally, we confirmed the main features of the proposed membrane topology in mammalian cells expressing full-length TRAM.

**MEMBRANE INSERTION AND TOPOLOGY OF THE
TRANSLOCATING CHAIN-ASSOCIATING MEMBRANE PROTEIN
(TRAM)**

Silvia Tamborero¹, Marçal Vilar², Luis Martínez-Gil¹, Arthur E. Johnson^{3,4,5} and Ismael Mingarro^{1*}

¹ Departament de Bioquímica i Biologia Molecular, Universitat de València. E-46 100 Burjassot, Spain. ² BCD-ND. Centro Nacional de Microbiología. ISCIII. Majadahonda, Spain. ³ Department of Molecular and Cellular Medicine, Texas A&M Health Science Center, College Station, TX 77843-1114. Departments of ⁴ Biochemistry and Biophysics and of ⁵ Chemistry, Texas A&M University, College Station, TX 77843, USA

* Corresponding author:

Phone: Int+34-963543796.

Fax: Int+34-963544635.

E-mail: Ismael.Mingarro@uv.es

Abstract

The translocating chain-associating membrane protein (TRAM) is a glycoprotein involved in the translocation of secreted proteins into the ER lumen, and in the insertion of integral membrane proteins into the lipid bilayer. As a major step toward elucidating the structure of the functional endoplasmic reticulum (ER) translocation/insertion machinery, we have characterized the membrane integration mechanism and the transmembrane (TM) topology of TRAM using two approaches: photocross-linking and truncated C-terminal reporter tag fusions. Our data indicate that TRAM is recognized by the signal recognition particle (SRP) and translocon components, and suggest a membrane topology with eight TM segments, including several poorly hydrophobic segments. Furthermore, we studied the membrane insertion capacity of these poorly hydrophobic segments into the ER membrane by themselves. Finally, we confirmed the main features of the proposed membrane topology in mammalian cells expressing full-length TRAM.

Keywords

membrane protein; topology; TRAM; photocrosslinking; translocon

Introduction

Protein insertion into or translocation across eukaryotic and prokaryotic membranes is a vital event in the biosynthesis of more than a third of the proteins in all living organisms. These processes are initiated by the signal recognition particle (SRP) targeting of secreted and integral membrane proteins to sites in the membrane termed translocons, where both translocation and integration occur. The translocons therefore function as two-way gates that direct hydrophilic protein regions across the membrane and hydrophobic transmembrane (TM) segments laterally into the lipid bilayer.

The translocon is a multi-protein complex composed of the Sec61 α , β and γ subunits and the translocating chain-associating membrane protein (TRAM)¹ in eukaryotic cells. Since translocon activity can be reproduced by *ab initio* reconstitution of these four membrane proteins in pure lipids², these proteins are considered to be the core components of the mammalian translocon³. The determination of the topology of the translocon components is essential for any understanding of the structure-function relationships of the translocon during translocation or integration. The membrane topology of the Sec61 α subunit was first determined in yeast using C-terminal reporter-domain fusions and protease digestions that suggested the presence of ten TM segments⁴. The crystal structure of the archeal homologue showed that the Sec61 α subunit consists of two domains of five TM segments each⁵, which forms a 'clam shell' structure that would provide a lateral gate for TM segments of nascent membrane proteins to partition into the lipid phase. Less information is available regarding the other translocon component, TRAM.

TRAM is a polytopic (multi-spanning) integral glycoprotein with an apparent size of 37 kDa involved early in the translocation of secreted proteins into the endoplasmic reticulum (ER) lumen^{1; 6}, and in the insertion of integral membrane proteins into the lipid bilayer^{2; 7; 8}. Based on a hydrophobicity analysis, TRAM is thought to span the ER

membrane eight times with both the N- and C-terminus facing the cytosol¹, although this model has not been experimentally verified.

In this study, we have used a photocrosslinking approach to determine the mechanism of TRAM insertion into the ER membrane. Our results establish that TRAM insertion involves SRP and the translocon. In addition, we report an experimental determination of the topology that TRAM acquires in ER membranes. *In vitro* translation of a series of TRAM truncations containing an *N*-linked glycosylation reporter tag identified the topological orientation of eight TM segments. Four of these TM segments are predicted to insert poorly into the membrane. In fact, two of these poorly hydrophobic TM segments failed to insert into the ER membrane by themselves, and their presence in the membrane suggest a functional role for TRAM during membrane protein biogenesis at the translocon. Finally, the main features of our *in vitro* experiments were confirmed by experiments using HEK293 cells expressing full-length TRAM.

Results

Cotranslational insertion of TRAM.

Integration of membrane proteins into ER-derived membranes can be monitored by glycosylation. This modification is performed by the oligosaccharyl transferase (OST) enzyme, which is adjacent to the translocon⁹. OST adds sugar residues cotranslationally to a consensus sequence after the protein emerges from the translocon pore. Glycosylation of a protein region translated *in vitro* in the presence of microsomal membranes therefore shows that this region of the nascent protein is exposed to the OST active site on the luminal side of the ER membrane. Glycosylation of a protein is detected by an increase in

molecular mass of about 2.5 kDa relative to the observed molecular mass of the protein expressed in the absence of microsomes.

When full-length TRAM was translated *in vitro* in reticulocyte lysate in the presence of rough microsomes (RM), much of the protein was glycosylated (Fig. 1a, lane 1). This result was further corroborated by treatment with endoglycosidase H (Fig. 1a, lane 2), a glycan-removing enzyme. Notably, when microsomal membranes were included post-translationally, after inhibition of protein biosynthesis with cycloheximide, the protein was not glycosylated (see Supplementary Fig. 1). The TRAM sequence contains three endogenous acceptor sites for *N*-linked glycosylation: N₅₆VT, N₁₂₀ES and N₃₅₅GT. No glycosylation was observed when the mutation N56Q of TRAM was expressed in the presence of RMs (Fig. 1b, lane 2). On the contrary, double mutant N120/355Q, with both the second and the third endogenous acceptor sites mutated, was efficiently glycosylated (Fig. 1b, lane 4). Therefore, the acceptor site N₅₆VT is cotranslationally glycosylated *in vitro*.

TRAM integrates into the ER membrane by interacting with SRP and translocon components.

Since the TRAM protein does not have a cleavable signal sequence, it seems likely that the first TM segment acts as a “signal-anchor” sequence that both targets the ribosome-nascent chain (RNC) complex to the translocon and also integrates into the ER membrane. To determine if ribosomes synthesizing TRAM are cotranslationally targeted to the ER membrane by the SRP, a previously described photocrosslinking technique was used^{10; 11; 12; 13}. Briefly, truncated TRAM mRNAs with an amber stop codon in the middle of the first putative TM segment were translated *in vitro* in wheat germ translation extracts in the presence of the amber suppressor aminoacyl-tRNA (ϵ ANB-Lys-tRNA^{amb}) and SRP. A translating ribosome halts when it reaches the end of an mRNA truncated in the coding

region, but the nascent chain does not dissociate from the tRNA-ribosome complex because the absence of a stop codon prevents normal termination from occurring. This translation mixture lacked microsomal membranes to avoid targeting the RNC-SRP intermediates to translocons. The translations were then photolyzed to initiate the photoreaction of the probe in the nascent chain with any nearby macromolecule.

To position the probe in the first TM segment of TRAM, its location was predicted using ΔG Prediction server (<http://dgpred.cbr.su.se>). The program predicts that the first TM segment comprises residues 24 through 44. The amber stop codon was therefore introduced at position 34 of the TRAM sequence (TAG34), approximately in the middle of the predicted TM region (Fig. 2a). We showed previously that a length of 55 residues between the photoreactive probe (TAG34) and the P-site at the ribosome (89-mer) was sufficient to ensure that the probe was outside the ribosomal exit tunnel and accessible for putative SRP binding^{12; 14}. When RNC complexes with 89-residue nascent chains were photolyzed, a prominent photoadduct was generated only in the presence of added SRP and ϵ ANB-Lys-tRNA^{amb}, but not in the presence of unmodified Lys-tRNA^{amb}. After UV illumination, a ~63 kDa photoadduct was formed when SRP and ϵ ANB-Lys-tRNA^{amb} were present (Fig. 2b, lane 4). In those cases where the photoreactive probe was not present or was substituted by unmodified Lys-tRNA^{amb}, no significant adduct was detected. The apparent molecular mass of this photoadduct corresponds to an adduct between SRP54 and the 89-residue nascent chain¹⁰. The first TM segment is therefore adjacent to the SRP54 subunit of SRP and apparently acts as a signal sequence to target the RNC complex to the translocon.

Because signal-anchor sequences are recognized twice, first by the SRP for targeting and subsequently by the translocon to initiate membrane insertion, we next sought to determine whether TRAM is adjacent to translocon components after targeting. To identify proteins adjacent to TRAM nascent chains during membrane insertion, integration

intermediates containing nascent TRAM chains of 109 residues (based on previous data ¹²) were prepared using microsomal membranes. As above, the photoactive probe was incorporated by translation of the truncated mRNAs with an amber codon at position 34 (TAG₃₄) in the presence of ϵ ANB-Lys-tRNA^{amb}. The 109-residue intermediate was photolyzed and the nature of the photoadducts analyzed by immunoprecipitation using affinity-purified antibodies to Sec61 α and TRAM itself (the anti-TRAM antibodies were raised against its 12-residue C-terminal peptide ⁸). The 109-residue intermediate consistently reacted covalently with Sec61 α (Fig. 2c, lane 2), but photocrosslinking to Sec61 α was not very efficient. A 109-residue integration intermediate was also immunoprecipitated in parallel using TRAM antibodies. In these experiments, the first TM segment of nascent TRAM was adjacent to a full-length TRAM molecule in the translocon generating a photoadduct with the apparent molecular mass of ~48 kDa (Fig. 2c, lane 3). Thus, the insertion of TRAM into the ER membrane takes place through the translocon complex.

To demonstrate that the integration of the TRAM constructs into the membrane is SRP dependent, TRAM nascent chains of 119 residues, which includes one *N*-linked glycosylation site that can be used as a “reporter” to follow membrane integration, were expressed in wheat germ in the presence of microsomes (Fig. 2d). Translation of this construct in wheat germ with rough microsomal membranes present cotranslationally showed glycosylation which was less efficient than for the reticulocyte translations (compare Fig. 2d lane 2 with Fig. 1a lane 1). This reduction in efficiency can be attributed to the different SRP levels in the two translation systems ¹⁵. In fact, addition of 20 nM SRP to the wheat germ translation significantly increased glycosylation of the TRAM construct (Fig. 2d, lanes 3 and 4). Therefore, SRP is not only adjacent but also required to target TRAM nascent polypeptides to the ER membrane.

Membrane Topology of TRAM in the ER membrane.

The membrane topology predicted for TRAM by the TM hidden Markov model method (TMHMM) ¹⁶ is shown in Fig. 3a. There are eight predicted TM helices with an N- and C-terminal cytoplasmic orientation. To experimentally determine the topology of TRAM, we used a glycosylation mapping approach ¹⁷ to identify the location of the N- and C-terminal ends of the protein and of the predicted loops relative to the ER membrane. Since the first TM segment is successfully recognized by the SRP and translocon components, and the first N-linked glycosylation acceptor site (N₅₆VT) is efficiently glycosylated, the first TM segment should span the membrane approximately from residue 24 to residue 44, as predicted by the Δ G Prediction server (see above). It has been reported previously that half-maximal glycosylation occurs when the acceptor Asn is ~12-14 residues away from the membrane ^{18; 19}. Therefore, since Asn56 is glycosylated (see Fig. 1), the first TM segment may extend up to Ala44, with the N-terminus oriented toward the cytoplasm.

The TM segments were tested by *in vitro* translation/insertion of a series of TRAM truncations containing native and, in the appropriate cases, an added N-linked glycosylation reporter tag. All the constructs used are shown on top of Figs. 3b and 4. As shown in Fig. 3b, translation products containing the first 119 residues of TRAM, including the first two predicted TM segments and a native glycosylation site (N₅₆VT), were efficiently glycosylated in the presence of RM, supporting translocation of the hydrophilic loop containing the glycosylation site. Truncated 129-mer polypeptides, which include the native potential glycosylation site located at position 120 (N₁₂₀ES), were singly glycosylated, indicating that the second predicted TM segment efficiently integrates into the membrane. Adding a C-terminal NST-tag (NSTMSM) to the 129-residue truncated polypeptide further corroborated this topology, since this construct (129-mer^Y) was singly-glycosylated in the

presence of RM (Fig. 3b, lane 6). The topology of these constructs was further supported by proteinase K experiments (see Supplementary Fig. 2).

Insertion of the third predicted TM segment was tested by translating a 166-residue truncation with the same (NSTMSM) C-terminal tag (166-mer^Y). The double glycosylation of this construct (Fig. 3b, lane 8) indicates that the third predicted TM segment was inserted and the C-terminal hydrophilic region was translocated into the lumen of the ER. Translation of a C-terminal tagged 196-mer^Y construct in the presence of RM resulted in singly-glycosylated forms (Fig. 4, lane 2), indicating that the predicted fourth TM segment was inserted.

According to the predicted membrane topology of TRAM, only three amino acid residues separate TM5 and TM6 (see Fig. 3a). Moreover, if the last predicted TM domain in the 217-mer^Y construct ends at residue 214, only four C-terminal amino acid residues protrude from the membrane. As noted above, 12-14 residues of a nascent chain protruding from the membrane are required to obtain half-maximal glycosylation. Therefore, to study this region of TRAM we tested two constructs, one with the C-terminal tag immediately after residue 217 (217-mer^Y), and a second one in which we added a flexible amino acid linker to extend the Asn glycosylation acceptor site further away from the membrane (217-mer^{=Y}). The amino acid sequence of this extended glycosylation tag was GGMGMGGMMNSTMSM. Translation/insertion *in vitro* of both constructs in the presence and in the absence of RM (Fig. 4, lanes 3-6) rendered singly and doubly-glycosylated forms for 217-mer^Y and 217-mer^{=Y}, respectively. These results together suggest that TM5 is in fact inserted into the membrane. Finally, translation/insertion experiments for 250-mer^Y and 292-mer^Y constructs show singly- and doubly-glycosylated forms respectively, suggesting the efficient insertion of TM6 in the 250-mer^Y construct and insertion of both TM6 and TM7 in the 292-mer^Y construct (Fig. 4, lanes 7-10).

Furthermore, the single glycosylation of the full-length TRAM protein, combined with the absence of glycosylation in the full-length N56Q mutant and the presence of a non-modified glycosylation acceptor site at N355 (Fig. 1), support the presence of an inserted eighth TM segment.

Membrane insertion of isolated TM segments.

Several of the putative TM segments of TRAM contain hydrophilic or even charged amino acid residues that, according to the present results, properly span the membrane in the fully assembled molecules. However, computer-assisted analysis of TRAM TM segments using the ΔG Prediction program show that TM segments 3, 4, 5 and 6 (almost all containing hydrophilic residues) would not integrate efficiently into the membrane (Table 1). In this algorithm a positive ΔG value (red numbering) is indicative of translocation, while a negative value (green numbering) indicates membrane integration.

To determine whether these segments insert into the membrane independently, we used an experimental system based on the *Escherichia coli* inner membrane protein leader peptidase (Lep) that detects the integration of TM helices into ER membranes²⁰. Lep consists of two TM segments connected by a cytoplasmic loop (P1) and a large C-terminal domain (P2), and inserts into ER-derived membranes with both termini located in the lumen (Fig. 5, top). The segment tested (TM-tested) is engineered into the luminal P2 domain and is flanked by two acceptor sites (G1 and G2) for *N*-linked glycosylation. In this system, single glycosylation of the protein denotes membrane integration of the segment being examined, while double glycosylation indicates translocation of the tested segment across the membrane. Quantification of the fractions of singly glycosylated (f_{1g}) and doubly glycosylated (f_{2g}) molecules makes it possible to calculate an apparent equilibrium constant, K_{app} , for the membrane insertion of a given TM-tested, $K_{app} = f_{1g}/f_{2g}$. The K_{app} value can be converted into the apparent free energy difference between the non-inserted state and the

inserted state using: $\Delta G_{app} = -RT \ln K_{app}$, where R is the gas constant ($R = 1.986$ kcal/K·mol) and T is the absolute temperature ($T = 303$ K).

Figure 5 shows the translation products of four separate constructs harboring TM3 (residues 124-142), TM4 (residues 167-185), TM5 (residues 197-214) or TM6 (residues 218-240) sequences in the presence of RM. When a construct containing TM3 sequence was assayed, 67% of the membrane-inserted Lep molecules were singly glycosylated (Fig. 5, lane 2), thereby indicating that TM3 is properly recognized for membrane insertion, even though its lower hydrophobicity. However, translation of two different constructs containing TM4 (<5% of insertion) or TM5 (8% of insertion) resulted in mainly doubly-glycosylated proteins (Fig. 5, lanes 4 and 6), suggesting that these isolated segments were translocated and not inserted into the bilayer. On the other hand, translation of a construct containing amino acids 218 to 240 (TM6) rendered a singly glycosylated population of 76% (Figure 5, lane 8), thus both TM3 and TM6 inserted unexpectedly well when tested in the Lep construct ($\Delta G_{app} < 0$, Table 1). These two helices have the lowest predicted ΔG_{app} of the investigated poorly hydrophobic TM segments ($\Delta G_{app}^{pred} = 0.3$ and 0.8 kcal/mol, respectively). Interestingly, ΔG_{app} for TM6 is -0.7 in our experiments compared to the predicted 0.8 kcal/mol. TM6 contains a charged residue towards the cytosolic end of the hydrophobic region, and it has been shown that positive charges of the cytosolic side of a TM helix can aid insertion in the Lep system²¹, as expected from the so-called “positive-inside” rule²².

It has been shown previously that in some cases, a neighboring TMH can favor the membrane insertion of poorly hydrophobic TM segments²³, especially in the case of the preceding TM segment²⁴. To investigate to what degree the insertion of a poorly inserted TM segment from TRAM can be affected by the presence of the preceding TM segment, we focused on TM4, because to facilitate the interpretation of the experimental results, it

was required that the preceding TM segment insert efficiently on its own (experimental $\Delta G_{app} < 0$ kcal/mol, see Table 1). Since this construct with two guest TM helices can give rise different theoretically possible topological forms, we engineered an additional glycosylation site at the loop connecting TM3 and TM4 (G3, see Fig. 6). This allowed us to achieve easily interpretable patterns for the construct containing TM3 + TM4. The native loop between the helices was retained to avoid potential artifacts from non-native sequence interactions. As seen in Fig. 6, protein constructs were triple glycosylated to 24%. This means that both helices were translocated into the microsomal lumen to this percentage. The fraction of the construct receiving only one glycan moiety, can result from either helix inserting into the membrane, while the other does not. However, by far it is most probable that TM3 is the inserted helix since it inserts to 67% on its own, while TM4 inserts to <5% when assayed independently (Fig. 5). Finally, doubly glycosylated forms arise from the insertion of both TM helices as a hairpin (15% of the molecules). Taken together, we conclude that the presence of TM3 causes a noticeable increase (from <5% to 15%) in the fraction of molecules with a membrane-inserted TM4 relative to what it would be expected from independent insertion by merely multiplying the individual insertion propensity.

TRAM topology in mammalian cells.

In order to confirm the topology of TRAM in mammalian cells, we fused the V5-epitope to the C-terminus of TRAM (TRAM-V5) and transfected HEK293 cells. The resulting TRAM constructs were subjected to Western blot analysis and visualized using a V5-specific antibody. Fig. 7 shows that both the wild type and the N56Q mutant of TRAM were expressed in transfected HEK293 cell lysates. Notably, TRAM was shown predominantly in a singly-glycosylated form (Fig. 7, lane 2), and the modified glycosylation site was further corroborated by the absence of glycosylation in the N56Q mutant (Fig. 7 lane 3). Control cells transfected with an empty vector were also included (Fig. 7, lane 1). Thus,

Asn56 is efficiently modified *in vivo* in eukaryotic cells suggesting that TRAM adopts the same topology *in vivo* as was observed *in vitro* using ER-derived membranes.

Discussion

To examine the biogenesis of a primary component of the ER translocation/insertion machinery, we have investigated the targeting and insertion of TRAM in eukaryotic membranes. TRAM does not have a cleaved amino-terminal signal sequence, but we have demonstrated here that the first TM segment functions as a signal sequence that must emerge from the ribosome to bind SRP and thereby enable nascent TRAM targeting to the membrane (Fig. 2). Site-directed photocrosslinking assays using TRAM nascent chains, with a probe introduced roughly in the middle of the first TM segment, showed a clear photoadduct with a molecular mass of ~63 kDa, in good agreement to the expected molecular mass for an adduct between the 89-residue nascent chain and SRP54, the 54 kDa subunit of SRP (Fig 2b). The formation of this covalent photoadduct was light-dependent, probe-dependent and stimulated by the presence of SRP. Furthermore, SRP-dependent targeting was demonstrated by translating TRAM nascent chains in wheat germ extracts that have only very low concentrations of functional SRP²⁵. The targeting of nascent 119-residue TRAM to the ER membrane was significantly stimulated by SRP in the wheat germ system, as shown by the *N*-linked glycosylation of a natural TRAM site that acts as a reporter for successful nascent chain translocation (Fig. 2d). Thus, TRAM molecules were efficiently targeted and translocated into ER-derived membranes, as detected by glycosylation, in the presence of added SRP.

During membrane protein biosynthesis, topogenic determinants (hydrophobic TM segments and their connecting loops) interact with translocon components to control the movement and topology of peptide domains in the ER lumen, the lipid bilayer and the

cytosol²⁶. TRAM is one of the translocon components that has been implicated in the translocation or integration of many, but not all, secreted or membrane proteins^{8; 11; 27; 28; 29; 30; 31}. Although the precise molecular details of the mechanisms of TRAM function in these processes have yet to be clearly defined, TRAM has been found adjacent to short hydrophobic sequences and to TM segments containing charged residues^{28; 30; 31; 32}. Therefore, TRAM was previously proposed to perform a TM chaperone-like role during the integration of non-optimal TM segments into the bilayer^{28; 31}. Our topological data support such a model for TRAM function because the insertion of TM regions of the protein with limited hydrophobicity (TM3, TM4, TM5 and TM6) into the bilayer may provide a site(s) for collecting poorly hydrophobic TM segments from nascent polypeptides, and to shielding their hydrophilic patches before they are partitioned into the lipid bilayer. Yet since insertion of some of these segments individually and out of their natural context failed (Fig. 5), preceding nascent chain TM segments are also presumably required to assist TM4 and TM5 integration into the bilayer. Consistent with this interpretation, our results show that the insertion efficiency of TM4, the less hydrophobic TM segment of TRAM, can be substantially increased by the presence of the well-inserting preceding TM3 (Fig. 6). Interestingly, recent work has shown that flanking loops and nearest-neighbour TM segments are sufficient to ensure the insertion of many marginally hydrophobic helices²⁴. More detailed studies of the individual TM segments of TRAM identified here can now be carried out to pinpoint the precise molecular basis for insertion efficiency in each case and its relevance for the insertion of full length TRAM.

The proposed topology of TRAM (Fig. 7, bottom) that relies on the use of C-terminal glycosylation tags as a new and rapid technique for mapping TM segments, provides a basis for the functional dissection of this essential translocon component. Whether TRAM can operate as a membrane insertase on its own, as does its bacterial

‘functional homologue’ YidC³³, is currently not known. We consider it more likely that TRAM is a component of the translocon that facilitates the bundling and collecting of poorly hydrophobic TM segments at a single location within or adjacent to the translocon. Interactions between the TM segments of nascent polypeptides and TRAM would presumably mediate this localization and provide an opportunity for the nascent chain TM segments to assemble themselves into an arrangement that would be stable upon final partitioning into the nonpolar lipid bilayer. Interestingly, nascent bacterial inner membrane proteins have been cross-linked to YidC TM3 during membrane protein insertion³⁴. Future experiments will have to unravel the mechanistic details of how this processing occurs in eukaryotic membrane protein biogenesis.

Materials and Methods

Enzymes and chemicals. All enzymes as well as plasmid pGEM1, RiboMAX SP6 RNA polymerase system and rabbit reticulocyte lysate were purchased from Promega (Madison, WI). The ER rough microsomes from dog pancreas, SRP and the wheat germ translation extracts were obtained from tRNA Probes (College Station, TX). The [³⁵S]Met/Cys and ¹⁴C-methylated markers were purchased from GE Healthcare. The restriction enzymes and endoglycosidase H were purchased from Roche Molecular Biochemicals. The DNA plasmid, RNA clean up, and PCR purification kits were from Qiagen (Hilden, Germany). The PCR mutagenesis kit, QuikChange was from Stratagene (La Jolla, CA). All the oligonucleotides were purchased from Thermo (Ulm, Germany).

Computer-assisted Analysis of TRAM sequence. Prediction of TM helices and membrane orientation (topology) of TRAM was done using TMHMM¹⁶ (<http://www.cbs.dtu.dk/services/TMHMM>). The analysis of TM insertion of hydrophobic

regions of the protein was performed using ΔG Prediction Server^{20; 35} (<http://www.cbr.su.se/DGpred/>).

DNA Manipulation. The full-length TRAM sequence was cloned from a mouse brain cDNA library provided by Dr. H. Mira (University of Valencia). The forward primer 5'-ATGGCGATTTCGCAAGAAGAGC-3', and the reverse primer, 5'-CTAAGAAGACTTCTCTTTCCTGC-3', were designed according to the 5' and 3' coding regions of the cDNA encoding for TRAM1 from *Mus musculus* (GenBank accession number NP082449). After PCR amplification, products were cloned into the pGEM1-T plasmid (Promega) for the *in vitro* transcription/insertion assays. For the membrane insertion of isolated TM segments TRAM TM3, TM4, TM5, TM6 and TM3+TM4 were independently amplified and introduced into the modified *E. coli* leader peptidase (Lep) sequence from the pGEM1 plasmid^{36; 37} using *SpeI/KpnI* sites. In the case of transfection of mammalian cells, the TRAM sequence was cloned into pcDNA3.1/V5-His TOPO TA vector (Invitrogen). Mutations of Asn56 and the double mutant Asn120/Asn355 to Gln were performed using the QuikChange mutagenesis kit from Stratagene (La Jolla, CA). All DNA manipulations were confirmed by sequencing of plasmid DNAs.

***In vitro* transcription and translation.** Full-length TRAM DNA was amplified directly from pGEM1-T plasmid. Alternatively, TRAM truncated constructs were obtained by using reverse primers at defined positions either with tandem translational stop codons at the 3' end or with an *N*-glycosylation tag followed by tandem stop codons. For an improved design of C-terminal glycosylation tags see reference³⁸.

In vitro transcription and translation were performed as previously reported¹³. After membrane pelleting samples were analyzed by SDS-PAGE, and gels were visualized on a Fuji FLA3000 phosphorimager using the ImageGauge software. Endoglycosidase H (Endo H) treatment was done as previously described³⁹. The membrane insertion efficiency of a

given guest segment (TM-tested) was calculated as the quotient between the fraction of singly glycosylated protein and the summed fraction of the singly glycosylated and doubly glycosylated protein forms. For segment with two TM regions (TM3+TM4) and three glycosylation acceptor sites, the protein fraction of a particular topology, with n glycans, was calculated as the intensity of the area of the n times glycosylated protein band divided by the summed intensities of the areas of all glycosylated protein bands.

Photocross-linking experiments. Truncated mRNAs were generated by PCR using different reverse primers that lacked a stop codon to obtain nascent chains of a specific length. PCR products were *in vitro* transcribed using purified SP6 RNA polymerase. Nascent chains of the TRAM polypeptide, with photoreactive groups at residue 34, were synthesized in a wheat germ cell-free translation system. For SRP photocross-linking experiments, *in vitro* translation (typically 50 μ l, 26 $^{\circ}$ C, 40 min) of 89-residue nascent chains was performed in the presence of 40 nM SRP, 100 μ Ci of [35 S]Met, and 32 pmol of ϵ ANB-Lys-tRNA^{amb} as before^{10; 12}. After translation, samples were irradiated for 20 min on ice using a 500 watt mercury arc lamp. Photolyzed samples were sedimented through a 130- μ l sucrose cushion [0.5 M sucrose, 20 mM HEPES (pH 7.5), 4 mM Mg(OAc)₂, 100 mM KOAc] using a TLA100 rotor (Beckman Instruments; 100,000 rpm; 4 min; 4 $^{\circ}$ C) to recover the RNC·SRP complexes. Pellets were resuspended in sample buffer before analysis by SDS-PAGE and detection by phosphorimaging as previously¹².

To assess Sec61 α and TRAM photocrosslinking, truncated mRNAs for 109-residue nascent chains were translated as described above but in the presence of 8 eq of column-washed rough ER microsomes. Samples were photolyzed and sedimented as above prior to sample immunoprecipitation. Pelleted membranes were resuspended and processed for Sec61 α or TRAM immunoprecipitation as recently detailed¹⁴.

Transfection of HEK293 cells. 10 μ g of TRAM-V5 wild type and mutant Asn56Gln encoding vector together with an empty control vector were transfected using the calcium-phosphate precipitation protocol. After 16 h of transfection cells were washed with PBS buffer and the media was changed. 48 h after transfection cells were washed with PBS, pooled and resuspended with lysis buffer (50 mM Tris-HCl pH 7.5, 100 mM NaCl, 1 mM EDTA, 0.1% SDS and a cocktail of protease inhibitors). Cell lysates were clarified by centrifugation and 40 μ g of total protein was used for SDS-PAGE and Western blot immunodetection using V5 antibody.

Acknowledgements

This work was supported by grants PR2008-0051 (Mobility Program) and BFU2009-08401(BMC) from the Spanish Ministry of Science and Innovation (MICINN, ERDF supported) and PROMETEO/2010/005 from the Generalitat Valenciana (to I.M.), and by NIH grant GM26494 and the Robert A. Welch Foundation chair grant BE-0017 (to A.E.J.). S.T. was recipient of a predoctoral fellowship from the University of Valencia (V Segles program). We are grateful to Ana Font for excellent technical assistance and to Helena Mira (Univ. of Valencia) for providing the cDNA library.

The abbreviations used are: OST, oligosaccharyl transferase; RM, rough microsomes; RNC, ribosome-nascent chain; SRP, signal recognition particle; TM, transmembrane; TRAM, translocating chain-associating membrane;

Figure legends

Fig. 1. TRAM is cotranslationally inserted into rough microsomes and glycosylated at residue Asn56. (a) Full-length TRAM was translated *in vitro* in rabbit reticulocyte lysate in the presence of [³⁵S]Met/Cys and rough microsomes (RM). Lane 2, samples were treated with endoglycosidase H (Endo H) prior to SDS-PAGE analysis. (b) TRAM-derived constructs translated in the absence (–) and in the presence (+) of RM, containing single mutant Asn56Gln (lanes 1 and 2) and double mutant Asn120Gln and Asn355Gln (lanes 3 and 4). Note that Asn56 is the only glycosylation acceptor sequon present in the double mutant construct. Bands of non-glycosylated protein are indicated by a white dot and glycosylated proteins are indicated by a black dot. Molecular weight markers are shown at the left.

Fig. 2. Targeting and integration of TRAM truncated nascent chains into ER membranes requires SRP and translocon components. (a) Structural organization of TRAM N-terminus region. (b) Photocrosslinking of [³⁵S]Met-labeled TRAM to SRP. A single photoreactive probe was incorporated by positioning an amber stop codon at position 34 (roughly in the middle of the first TM segment). RNCs containing radioactive 89-residue nascent chains were prepared in wheat germ. Samples in lanes 2 and 4 were supplemented with exogenous SRP (40 nM). The band corresponding to a photoadduct between SRP54 and the 89-residue nascent chain is indicated by a black triangle. (c) Photocrosslinking of TRAM nascent chains to translocon components. For Sec61 α and TRAM experiments, after photolysis in the presence of membranes, an aliquot from each 109-residue RNC complex sample was removed and directly analyzed by SDS/PAGE to detect and normalize the total radioactive translation products (lane 1, labeled as totals). The remaining samples were split for IPs with Sec61 α (lane 2) and TRAM (lane 3) antisera. Major photoadducts identified by immunoprecipitation with antibodies specific for

Sec61 α and TRAM are highlighted with a downward and upward triangle, respectively. (d) SRP stimulates glycosylation. Translation of 119-residue nascent chain in a wheat germ system in the absence (lane 2) or in the presence (lane 3) of added SRP. The nature of the higher molecular weight bands was verified by endoglycosidase H (EndoH) treatment (lane 4). Bands of non-glycosylated forms are indicated by a white dot and glycosylated polypeptides are indicated by a black dot.

Fig. 3. (a) Topology prediction for full-length TRAM using the TMHMM prediction method. TM segments with the predicted residues, as well as the cytoplasmic and luminal loops, are indicated above the curves that show the *a posteriori* probabilities for the different locations. **(b)** *In vitro* expression and representative SDS-PAGE analysis of TRAM truncates. Structural organization of full-length and truncated TRAM constructs (top), with the C-terminal glycosylation tags shown as rectangles and the glycosylation sites denoted by Y symbols. Models of the membrane topology of truncated TRAM constructs are illustrated (bottom).

Fig. 4. Alternating orientation of TRAM TM segments. *In vitro* translation of truncated TRAM constructs in which a fused C-terminal *N*-glycosylation tag provides a simple readout for topology. Representative SDS-PAGE gels of relevant constructs are shown. Constructs were transcribed and translated in the presence or in the absence (as a control translation) of membranes as indicated. Structural organization and models for membrane topology of these truncated polypeptides are shown above and below, respectively.

Fig. 5. Insertion of isolated TM segments into microsomal membranes. Top, schematic representation of the Lep construct used to report insertion into ER membrane of poorly hydrophobic TRAM TM segments. The TM segment under study (TM-tested) is inserted into the P2 domain of Lep flanked by two artificial glycosylation acceptor sites (G1 and G2). Recognition of the tested sequence by the translocon machinery as a TM domain

locates only G1 in the luminal side of the ER membrane preventing G2 glycosylation. The Lep chimera will be doubly glycosylated when the sequence being tested is translocated into the lumen of the microsomes. The apparent free energy of membrane insertion (ΔG_{app}) of the TM segment in question (TM-tested) is quantified by comparing the fractions of singly and doubly glycosylated molecules, as described in the main text. Bottom, *in vitro* translation of different Lep constructs containing TRAM TM3, TM4, TM5 or TM6 in the presence of membranes. Constructs were transcribed and translated in the presence or in the absence of membranes as indicated. Bands of non-glycosylated protein are indicated by a white dot; singly and doubly glycosylated proteins are indicated by one and two black dots, respectively.

Fig. 6. Analysis of TM3 + TM4 insertion using a Lep variant with three glycosylation sites. Analogous to the integration of an isolated TM segment (Fig. 5), a TRAM fragment from residue Gln124 to Phe185 was introduced as TM-tested into Lep vector. To be able to distinguish the theoretically possible topologies, an additional glycosylation acceptor site (G3) was introduced in the loop connecting both TM segments by mutating Phe163 to Asn. Top, representative SDS-PAGE gel of the Lep variant with three glycosylation acceptor sites expressed in rabbit reticulocyte lysate in the presence (+RM) or absence (-RM) of dog pancreas microsomes. Bands of non-glycosylated protein are indicated by a white dot; singly, doubly and triply glycosylated proteins are indicated by one, two and three black dots, respectively. Bottom, all theoretically possible topologies are shown, but for those topologies compatible with only one of the two TM segments spanning the membrane, the topology where TM3 is translocated and TM4 inserted was considered improbable, as explained in the main text.

Fig. 7. Glycosylation of TRAM expressed in HEK293 cells. Analysis of TRAM glycosylation in transient transfected HEK293 cells with a plasmid encoding TRAM-V5

full-length wild type sequence (lane 2) and carrying the mutation Asn56Gln (lane 3). Lane 1 represents the transfection with an empty vector construct, as a control. Membrane topology model of full-length TRAM protein consistent with our data is illustrated at the bottom.

References

1. Görlich, D., Hartmann, E., Prehn, S. & Rapoport, T. A. (1992). A Protein of the Endoplasmic Reticulum Involved Early in Polypeptide Translocation. *Nature* **357**, 47-52.
2. Görlich, D. & Rapoport, T. A. (1993). Protein translocation into proteoliposomes reconstituted from purified components of the endoplasmic reticulum membrane. *Cell* **75**, 615-630.
3. Alder, N. N. & Johnson, A. E. (2004). Cotranslational membrane protein biogenesis at the endoplasmic reticulum. *J Biol Chem* **279**, 22787-90.
4. Wilkinson, B. M., Critchley, A. J. & Stirling, C. J. (1996). Determination of the transmembrane topology of yeast Sec61p, an essential component of the endoplasmic reticulum translocation complex. *J Biol Chem* **271**, 25590-25597.
5. Van den Berg, B., Clemons, W. M., Jr., Collinson, I., Modis, Y., Hartmann, E., Harrison, S. C. & Rapoport, T. A. (2004). X-ray structure of a protein-conducting channel. *Nature* **427**, 36-44.
6. Krieg, U. C., Johnson, A. E. & Walter, P. (1989). Protein Translocation Across the Endoplasmic Reticulum Membrane - Identification by Photocross-Linking of a 39-Kd Integral Membrane Glycoprotein As Part of a Putative Translocation Tunnel. *J Cell Biol* **109**, 2033-2043.
7. Thrift, R. N., Andrews, D. W., Walter, P. & Johnson, A. E. (1991). A Nascent Membrane Protein Is Located Adjacent to ER Membrane Proteins Throughout Its Integration and Translation. *J Cell Biol* **112**, 809-821.
8. Do, H., Falcone, D., Lin, J., Andrews, D. W. & Johnson, A. E. (1996). The cotranslational integration of membrane proteins into the phospholipid bilayer is a multistep process. *Cell* **85**, 369-378.
9. Nilsson, I., Kelleher, D. J., Miao, Y., Shao, Y., Kreibich, G., Gilmore, R., von Heijne, G. & Johnson, A. E. (2003). Photocross-linking of nascent chains to the STT3 subunit of the oligosaccharyltransferase complex. *J Cell Biol* **161**, 715-25.
10. Krieg, U. C., Walter, P. & Johnson, A. E. (1986). Photocrosslinking of the signal sequence of nascent preprolactin to the 54-kilodalton polypeptide of the signal recognition particle. *Proc Natl Acad Sci Usa* **83**, 8604-8.
11. McCormick, P. J., Miao, Y., Shao, Y., Lin, J. & Johnson, A. E. (2003). Cotranslational protein integration into the ER membrane is mediated by the binding of nascent chains to translocon proteins. *Mol Cell* **12**, 329-41.

12. Sauri, A., Saksena, S., Salgado, J., Johnson, A. E. & Mingarro, I. (2005). Double-spanning Plant Viral Movement Protein Integration into the Endoplasmic Reticulum Membrane Is Signal Recognition Particle-dependent, Translocon-mediated, and Concerted. *J Biol Chem* **280**, 25907-25912.
13. Sauri, A., Tamborero, S., Martinez-Gil, L., Johnson, A. E. & Mingarro, I. (2009). Viral membrane protein topology is dictated by multiple determinants in its sequence. *J Mol Biol* **387**, 113-28.
14. Martinez-Gil, L., Johnson, A. E. & Mingarro, I. (2010). Membrane insertion and biogenesis of the Turnip crinkle virus p9 movement protein. *J Virol* **84**, 5520-7.
15. Kanner, E. M., Klein, I. K., Friedlander, M. & Simon, S. M. (2002). The amino terminus of opsin translocates "posttranslationally" as efficiently as cotranslationally. *Biochemistry* **41**, 7707-15.
16. Krogh, A., Larsson, B., von Heijne, G. & Sonnhammer, E. L. (2001). Predicting transmembrane protein topology with a hidden Markov model: application to complete genomes. *J Mol Biol* **305**, 567-80.
17. Nilsson, I. M. & von Heijne, G. (1990). Fine-tuning the Topology of a Polytopic Membrane Protein. Role of Positively and Negatively Charged Residues. *Cell* **62**, 1135-1141.
18. Nilsson, I. & von Heijne, G. (1993). Determination of the distance between the oligosaccharyltransferase active site and the endoplasmic reticulum membrane. *J Biol Chem* **268**, 5798-5801.
19. Orzaez, M., Salgado, J., Gimenez-Giner, A., Perez-Paya, E. & Mingarro, I. (2004). Influence of proline residues in transmembrane helix packing. *J Mol Biol* **335**, 631-40.
20. Hessa, T., Kim, H., Bihlmaier, K., Lundin, C., Boekel, J., Andersson, H., Nilsson, I., White, S. H. & von Heijne, G. (2005). Recognition of transmembrane helices by the endoplasmic reticulum translocon. *Nature* **433**, 377-81.
21. Lerch-Bader, M., Lundin, C., Kim, H., Nilsson, I. & von Heijne, G. (2008). Contribution of positively charged flanking residues to the insertion of transmembrane helices into the endoplasmic reticulum. *Proc Natl Acad Sci U S A* **105**, 4127-32.
22. von Heijne, G. (1992). Membrane protein structure prediction - Hydrophobicity analysis and the positive-Inside rule. *J Mol Biol* **225**, 487-494.
23. Enquist, K., Fransson, M., Boekel, C., Bengtsson, I., Geiger, K., Lang, L., Pettersson, A., Johansson, S., von Heijne, G. & Nilsson, I. (2009). Membrane-integration characteristics of two ABC transporters, CFTR and P-glycoprotein. *J Mol Biol* **387**, 1153-64.
24. Hedin, L. E., Ojemalm, K., Bernsel, A., Hennerdal, A., Illergard, K., Enquist, K., Kauko, A., Cristobal, S., von Heijne, G., Lerch-Bader, M., Nilsson, I. & Elofsson, A. (2010). Membrane insertion of marginally hydrophobic transmembrane helices depends on sequence context. *J Mol Biol* **396**, 221-9.
25. Walter, P. & Blobel, G. (1981). Translocation of proteins across the endoplasmic reticulum III. Signal recognition protein (SRP) causes signal sequence-dependent and site-specific arrest of chain elongation that is released by microsomal membranes. *J Cell Biol* **91**, 557-61.
26. Skach, W. R. (2007). The expanding role of the ER translocon in membrane protein folding. *J Cell Biol* **179**, 1333-5.
27. Sauri, A., McCormick, P. J., Johnson, A. E. & Mingarro, I. (2007). Sec61alpha and TRAM are sequentially adjacent to a nascent viral membrane protein during its ER integration. *J Mol Biol* **366**, 366-74.

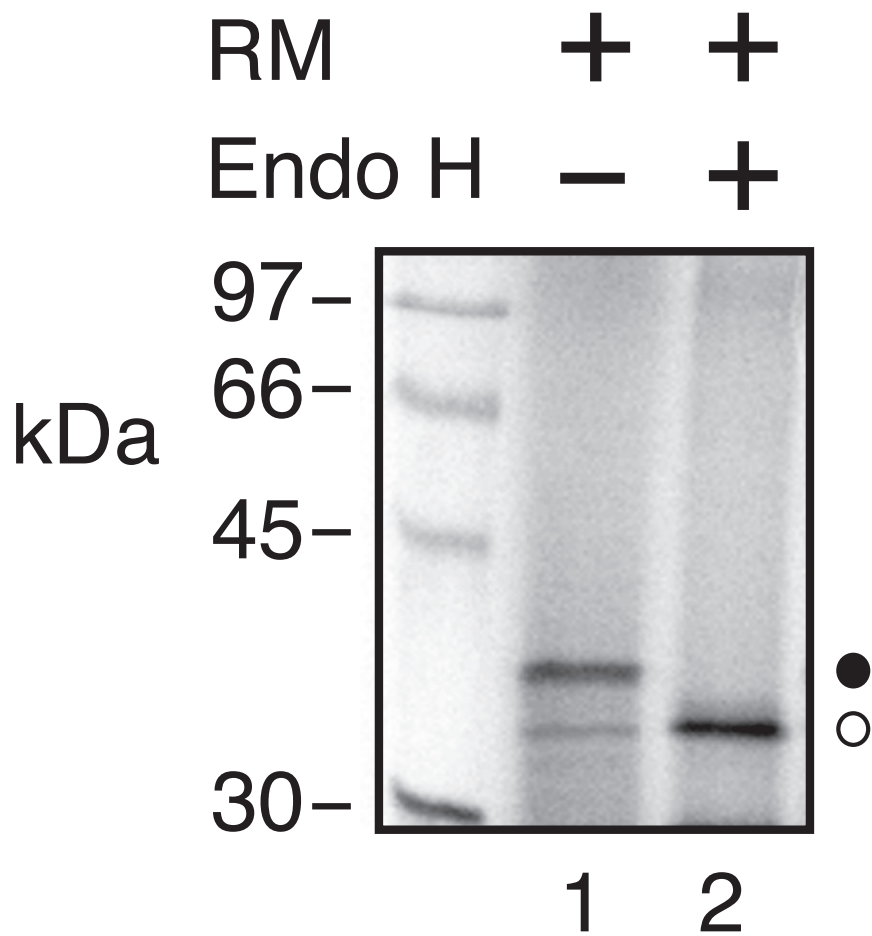
28. Cross, B. C. & High, S. (2009). Dissecting the physiological role of selective transmembrane-segment retention at the ER translocon. *J Cell Sci* **122**, 1768-77.
29. Heinrich, S. U. & Rapoport, T. A. (2003). Cooperation of transmembrane segments during the integration of a double-spanning protein into the ER membrane. *Embo J* **22**, 3654-63.
30. Voigt, S., Jungnickel, B., Hartmann, E. & Rapoport, T. A. (1996). Signal sequence-dependent function of the TRAM protein during early phases of protein transport across the endoplasmic reticulum membrane. *J Cell Biol* **134**, 25-35.
31. Heinrich, S. U., Mothes, W., Brunner, J. & Rapoport, T. A. (2000). The Sec61p complex mediates the integration of a membrane protein by allowing lipid partitioning of the transmembrane domain. *Cell* **102**, 233-44.
32. Meacock, S. L., Lecomte, F. J., Crawshaw, S. G. & High, S. (2002). Different transmembrane domains associate with distinct endoplasmic reticulum components during membrane integration of a polytopic protein. *Mol Biol Cell* **13**, 4114-29.
33. Dalbey, R. E. & Kuhn, A. (2004). YidC family members are involved in the membrane insertion, lateral integration, folding, and assembly of membrane proteins. *J Cell Biol* **166**, 769-74.
34. Yu, Z., Koningstein, G., Pop, A. & Luirink, J. (2008). The conserved third transmembrane segment of YidC contacts nascent Escherichia coli inner membrane proteins. *J Biol Chem* **283**, 34635-42.
35. Hessa, T., Meindl-Beinker, N. M., Bernsel, A., Kim, H., Sato, Y., Lerch-Bader, M., Nilsson, I., White, S. H. & von Heijne, G. (2007). Molecular code for transmembrane-helix recognition by the Sec61 translocon. *Nature* **450**, 1026-30.
36. Saaf, A., Wallin, E. & von Heijne, G. (1998). Stop-transfer function of pseudo-random amino acid segments during translocation across prokaryotic and eukaryotic membranes. *Eur J Biochem* **251**, 821-9.
37. Martinez-Gil, L., Perez-Gil, J. & Mingarro, I. (2008). The surfactant peptide KL4 sequence is inserted with a transmembrane orientation into the endoplasmic reticulum membrane. *Biophys J* **95**, L36-8.
38. Bano-Polo, M., Baldin, F., Tamborero, S., Marti-Renom, M. A. & Mingarro, I. (2011). N-glycosylation efficiency is determined by the distance to the C-terminus and the amino acid preceding an Asn-Ser-Thr sequon. *Protein Sci* **20**, 179-86.
39. Martinez-Gil, L., Sauri, A., Vilar, M., Pallas, V. & Mingarro, I. (2007). Membrane insertion and topology of the p7B movement protein of Melon Necrotic Spot Virus (MNSV). *Virology* **367**, 348-57.

Table 1. Apparent free energies of the hydrophobic regions of TRAM

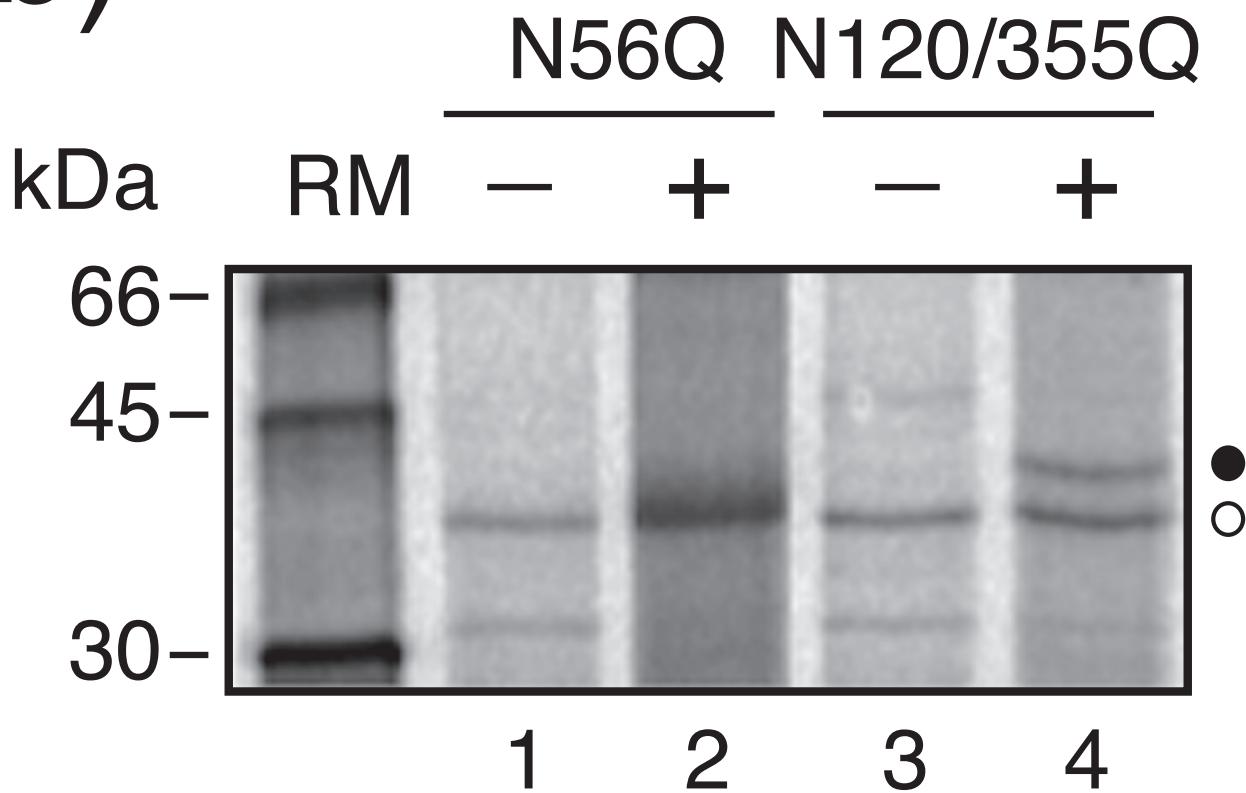
Hydrophobic region	Sequence	pred ΔG_{app}	ΔG_{app}
TM1	²⁴ ADIVSCLAMLFLGLMFEVTA ⁴⁴	-0.6	
TM2	⁸⁰ LATVLFYMLVAIIHAIHQEYVL ¹⁰²	-1.2	
TM3	¹²⁴ QLSAFYLFACVWGTFILIS ¹⁴²	0.3	-0.4
TM4	¹⁶⁷ FFYISQLAYWLHAFPELYF ¹⁸⁵	4.0	1.3
TM5	¹⁹⁷ LVYIGLYLFHIAGAYLLN ²¹⁴	1.1	1.1
TM6	²¹⁸ LGLVLLVLHYFVEFLFHISRLFY ²⁴⁰	0.8	-0.7
TM7	²⁵² LWAVLFVLGRLLTLILSVLTVGF ²⁷⁴	-1.1	
TM8	²⁹³ VLAVRIAVLASICITQAFMMWKFI ³¹⁶	-0.6	

Predicted values for the insertion efficiency of TRAM hydrophobic regions using the biological hydrophobicity scale (ΔG_{app}^{pred}), and experimentally determined values for apparent free energies (ΔG_{app}) of poorly hydrophobic helices from the *in vitro* glycosylation assay (in kcal/mol). Each segment was introduced as a TM-tested into the Lep vector, and ΔG_{app} values were obtained as described in the main text. Positive ΔG_{app} values, indicative of membrane translocation are shown in red.

Figure 1
(a)



(b)



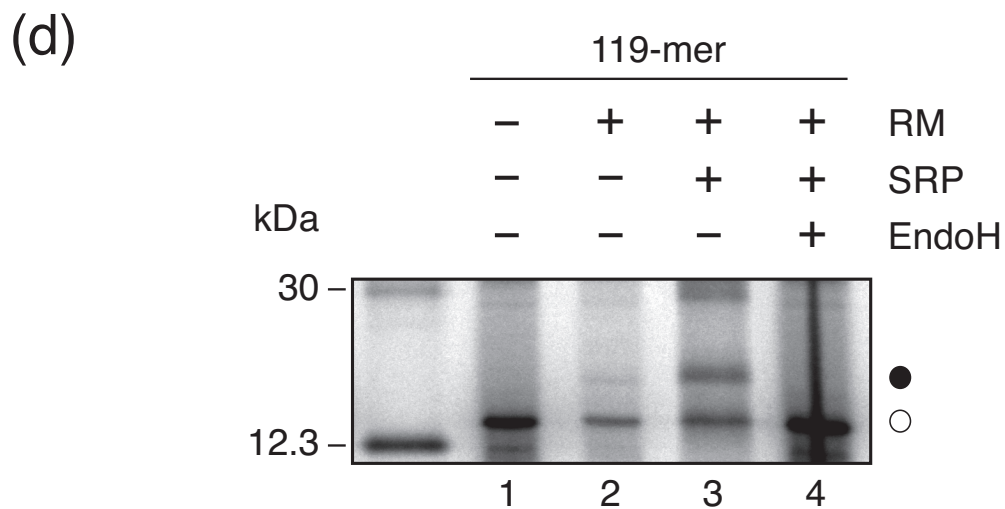
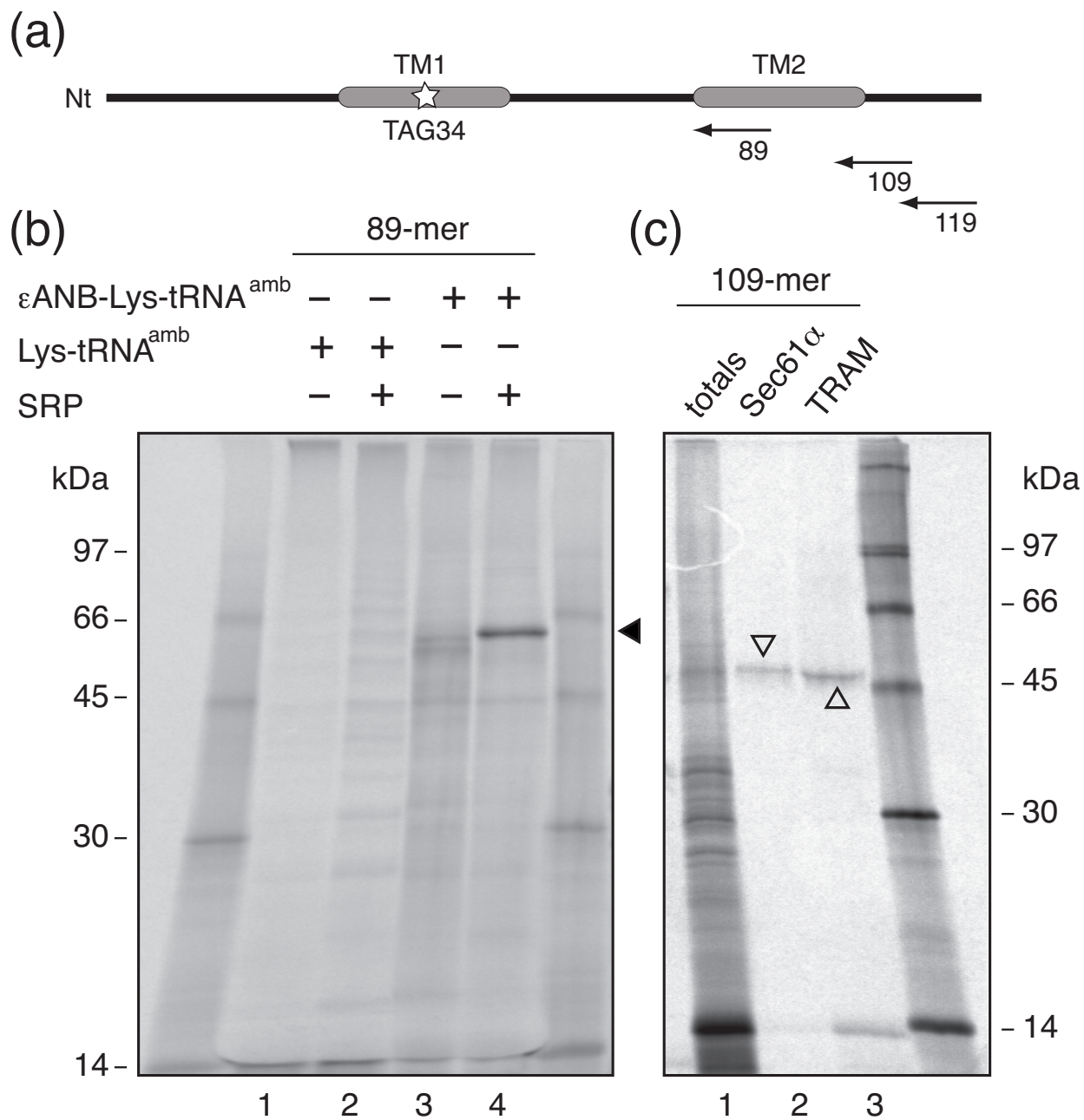


Figure 3

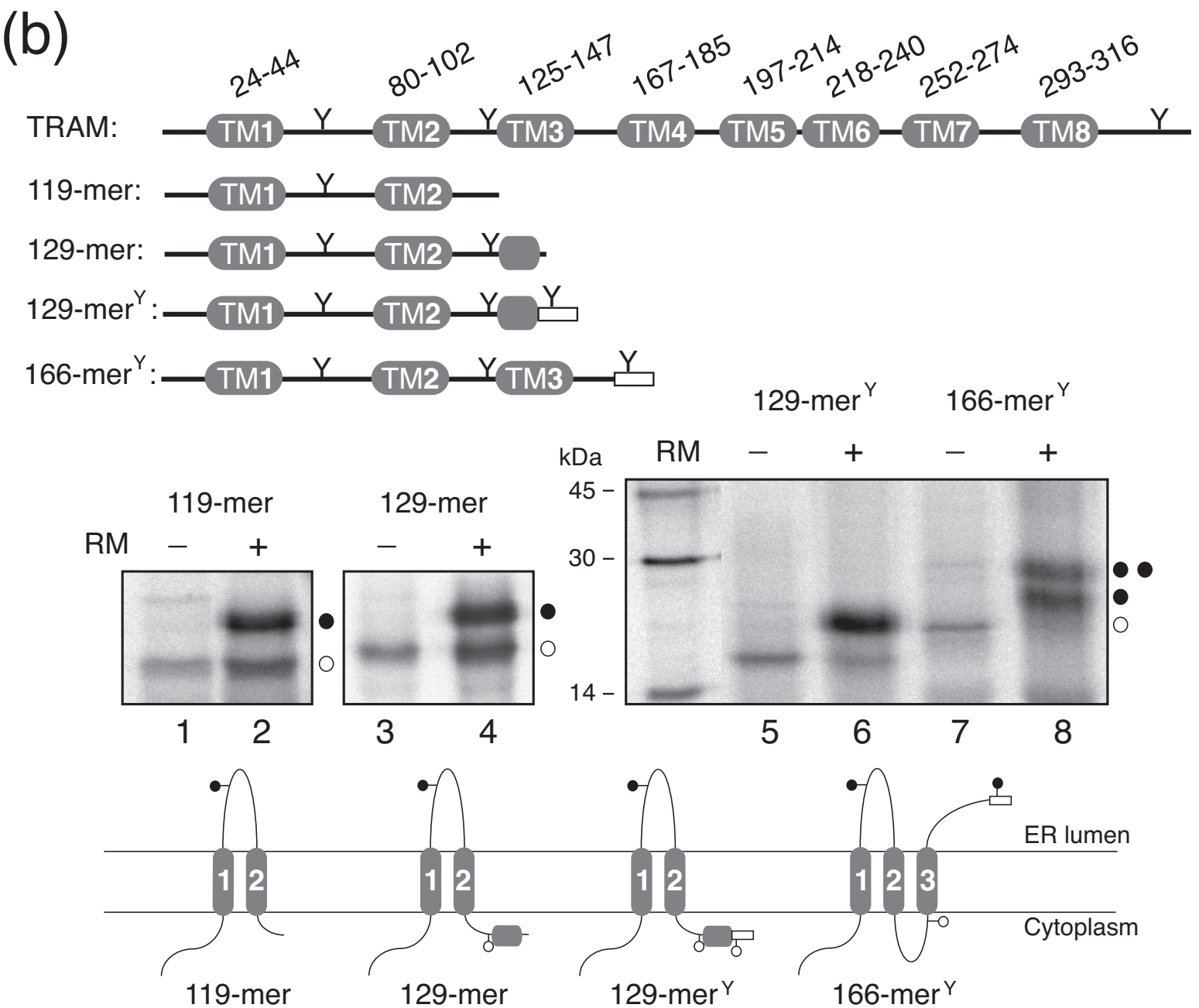
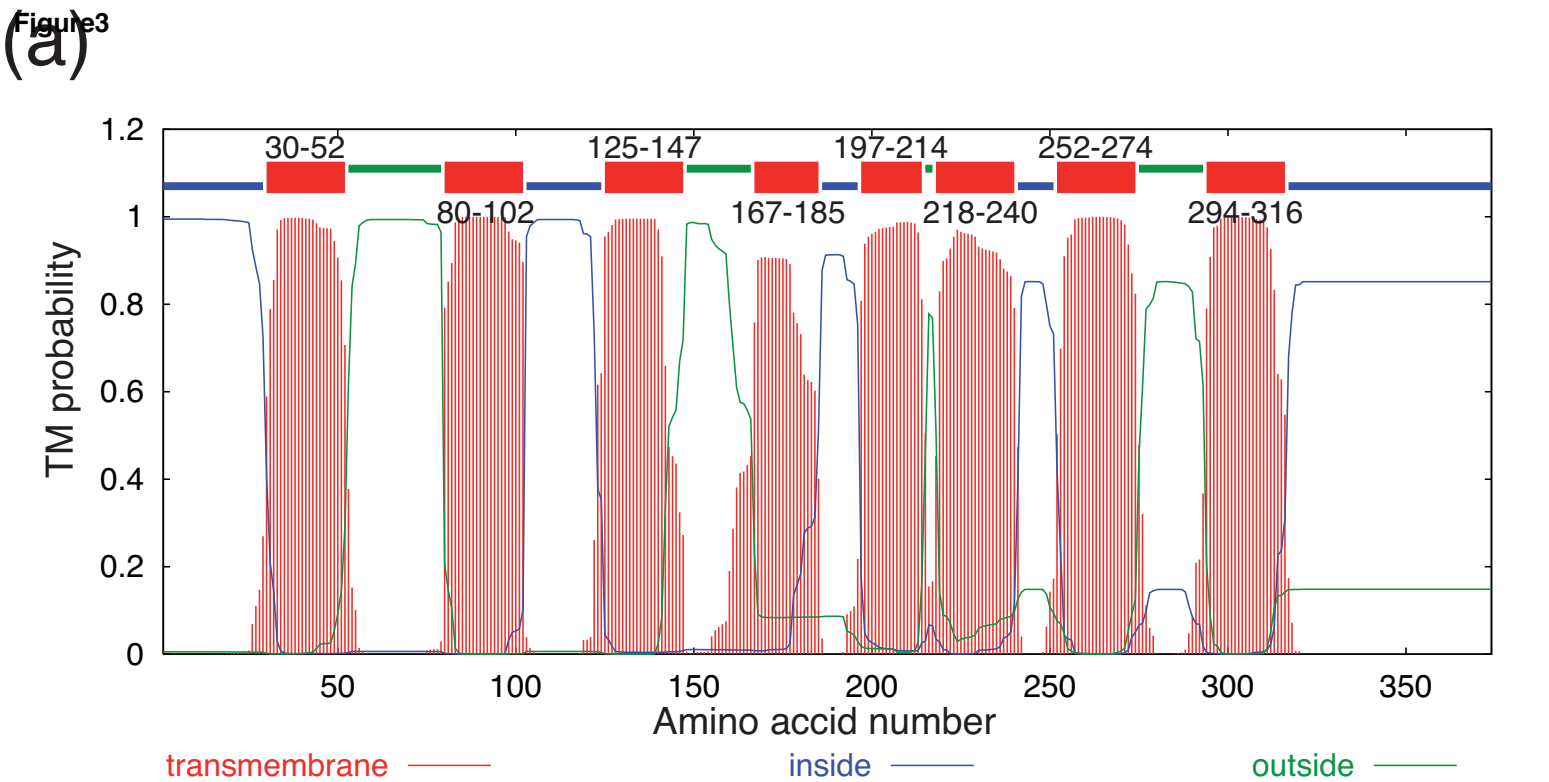


Figure 4

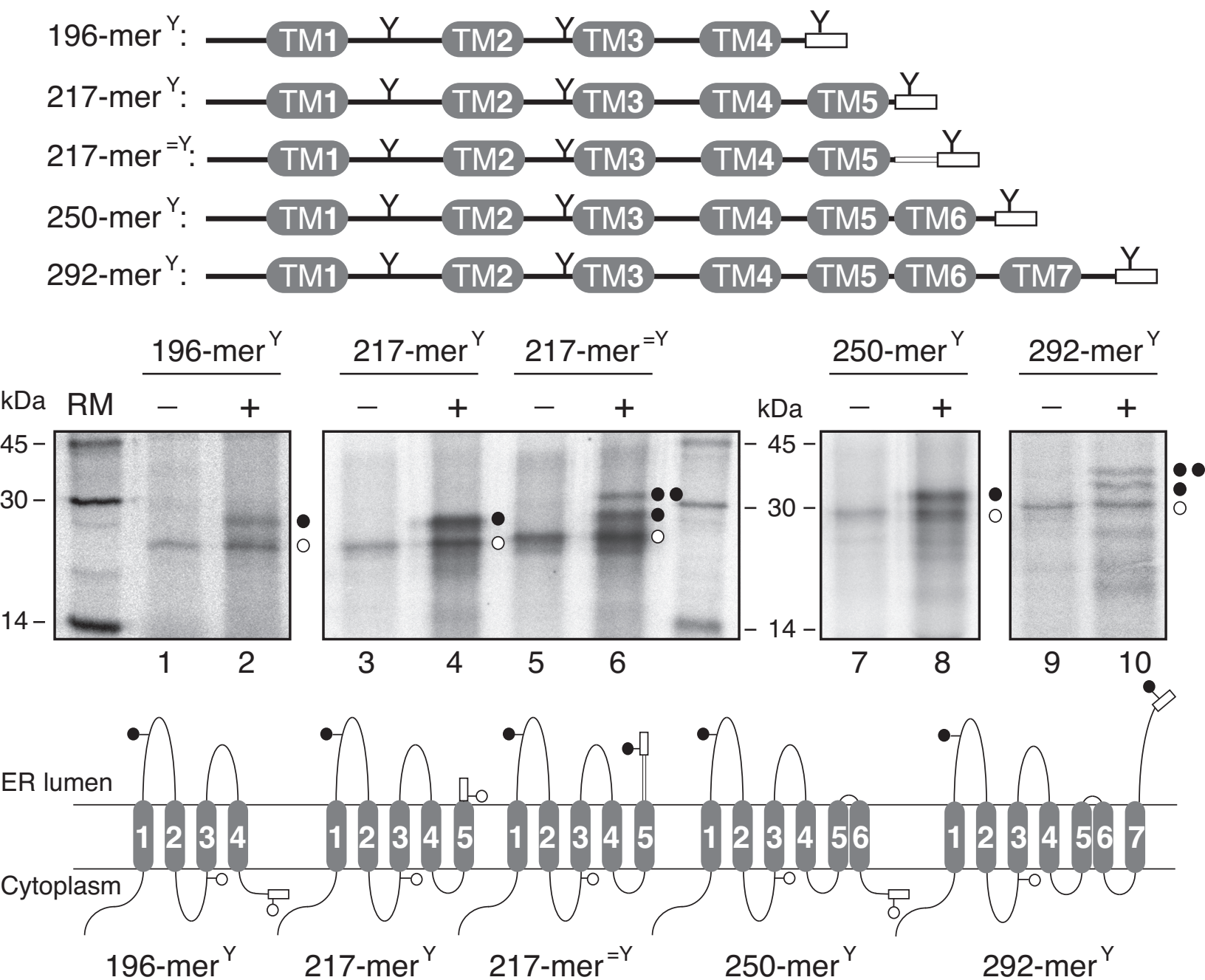
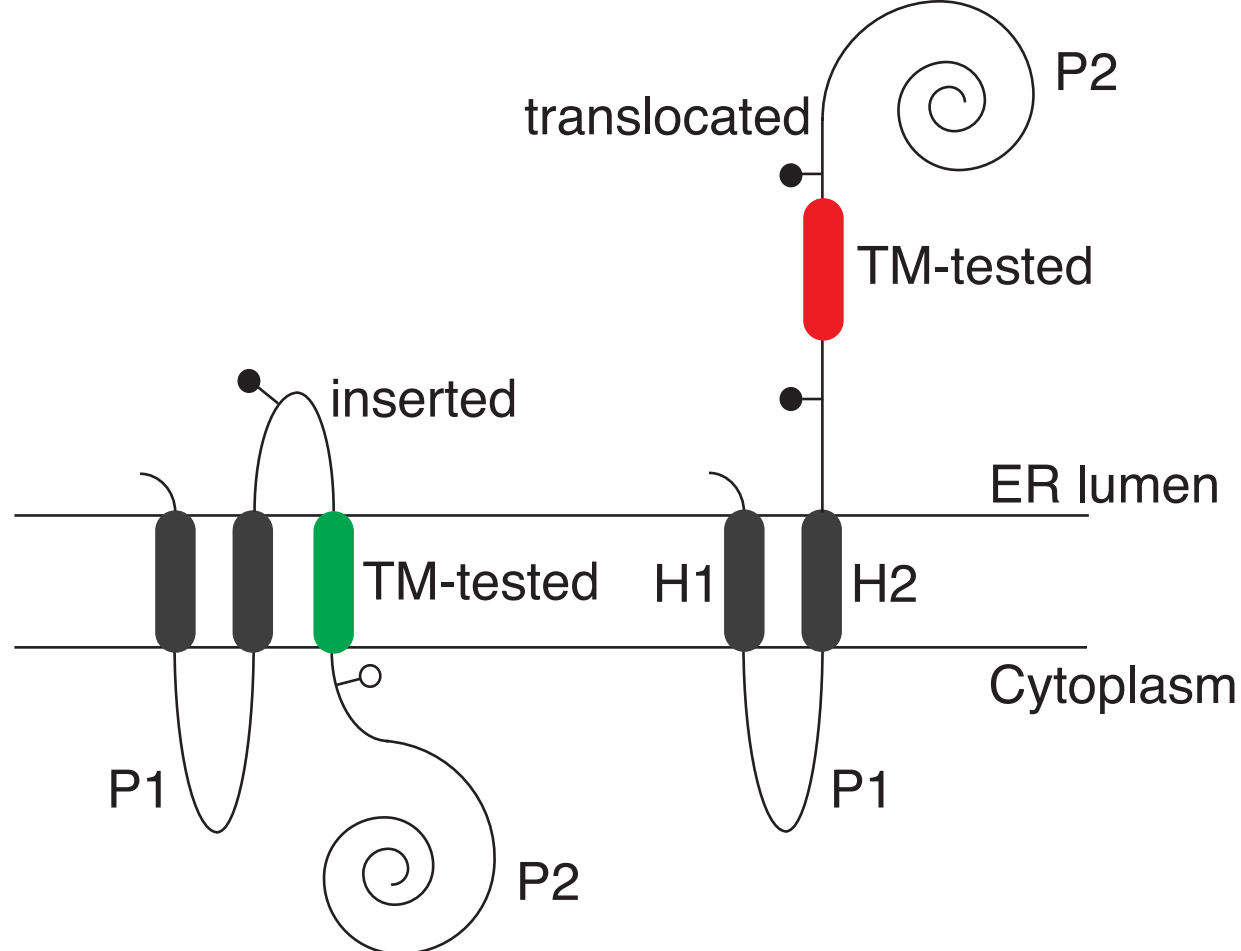


Figure 5



	TM3		TM4		TM5		TM6	
RM	-	+	-	+	-	+	-	+

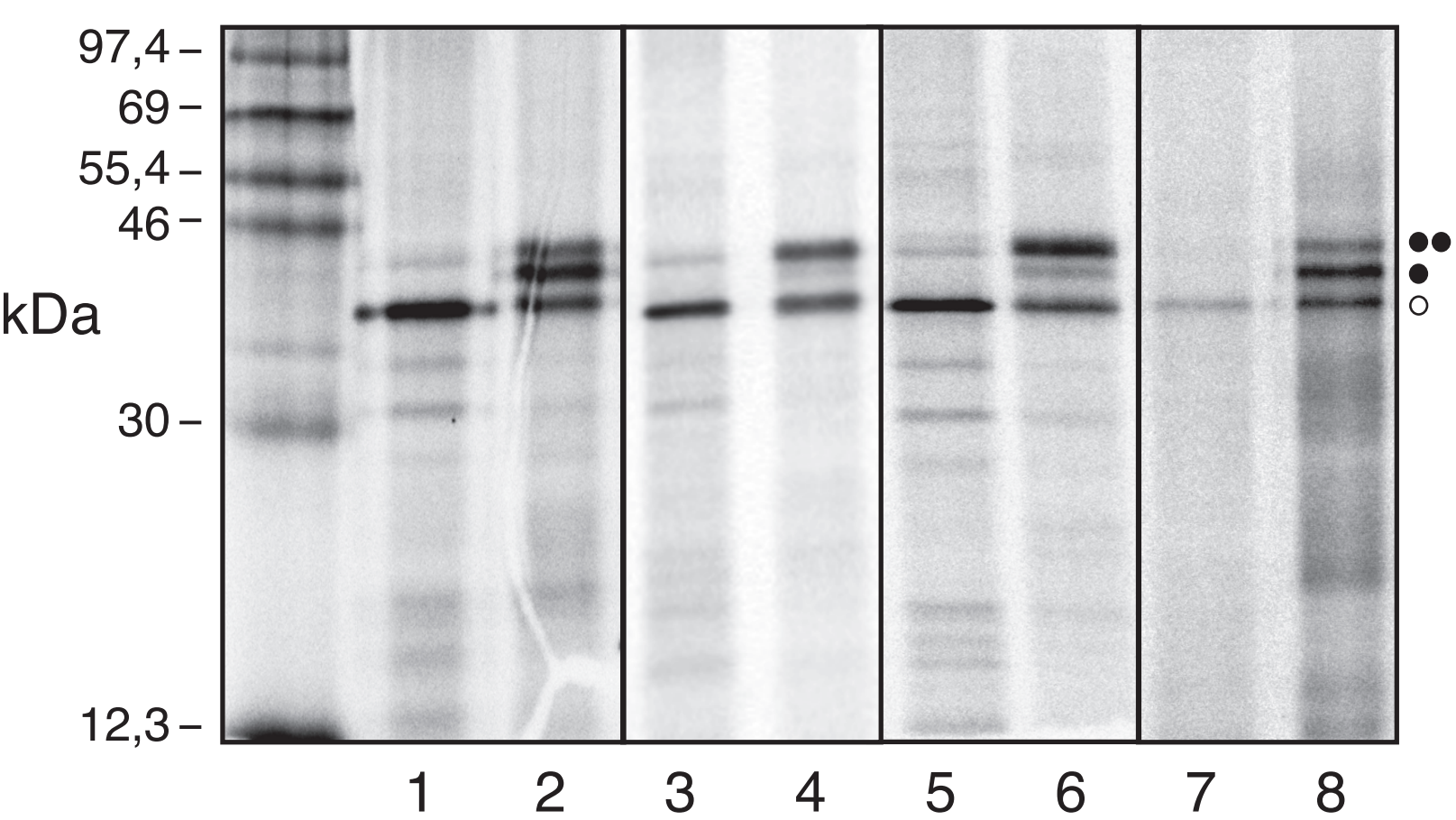


Figure 6

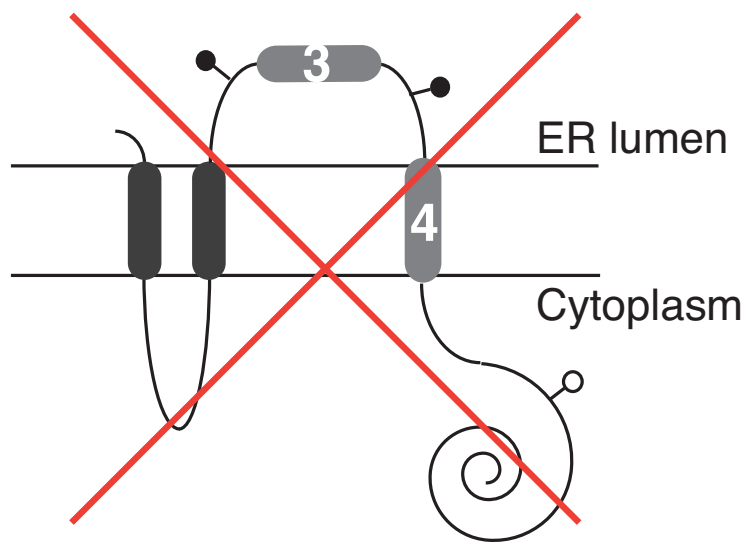
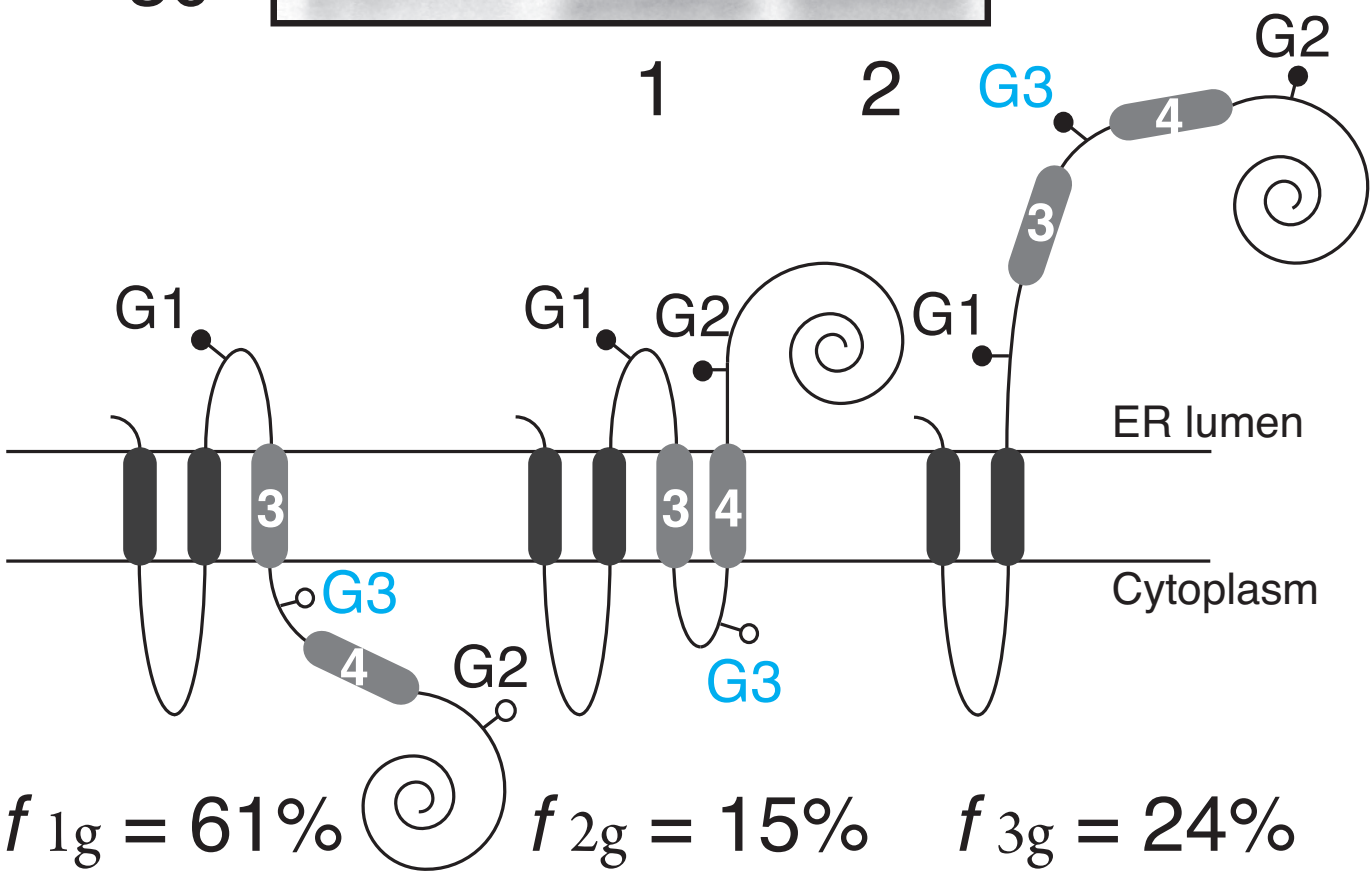
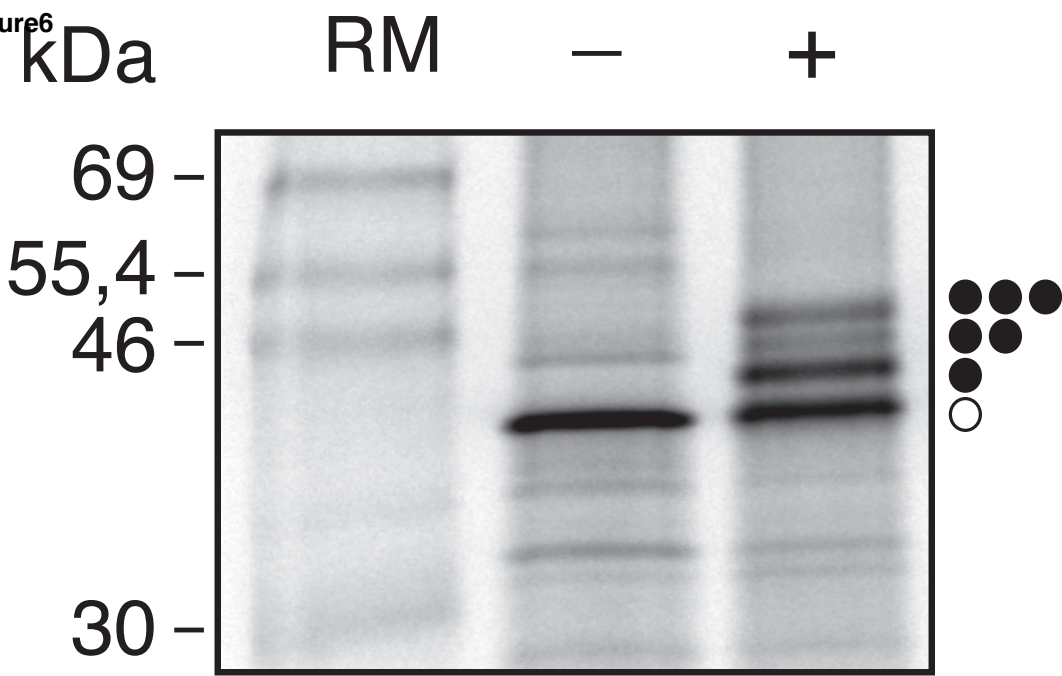
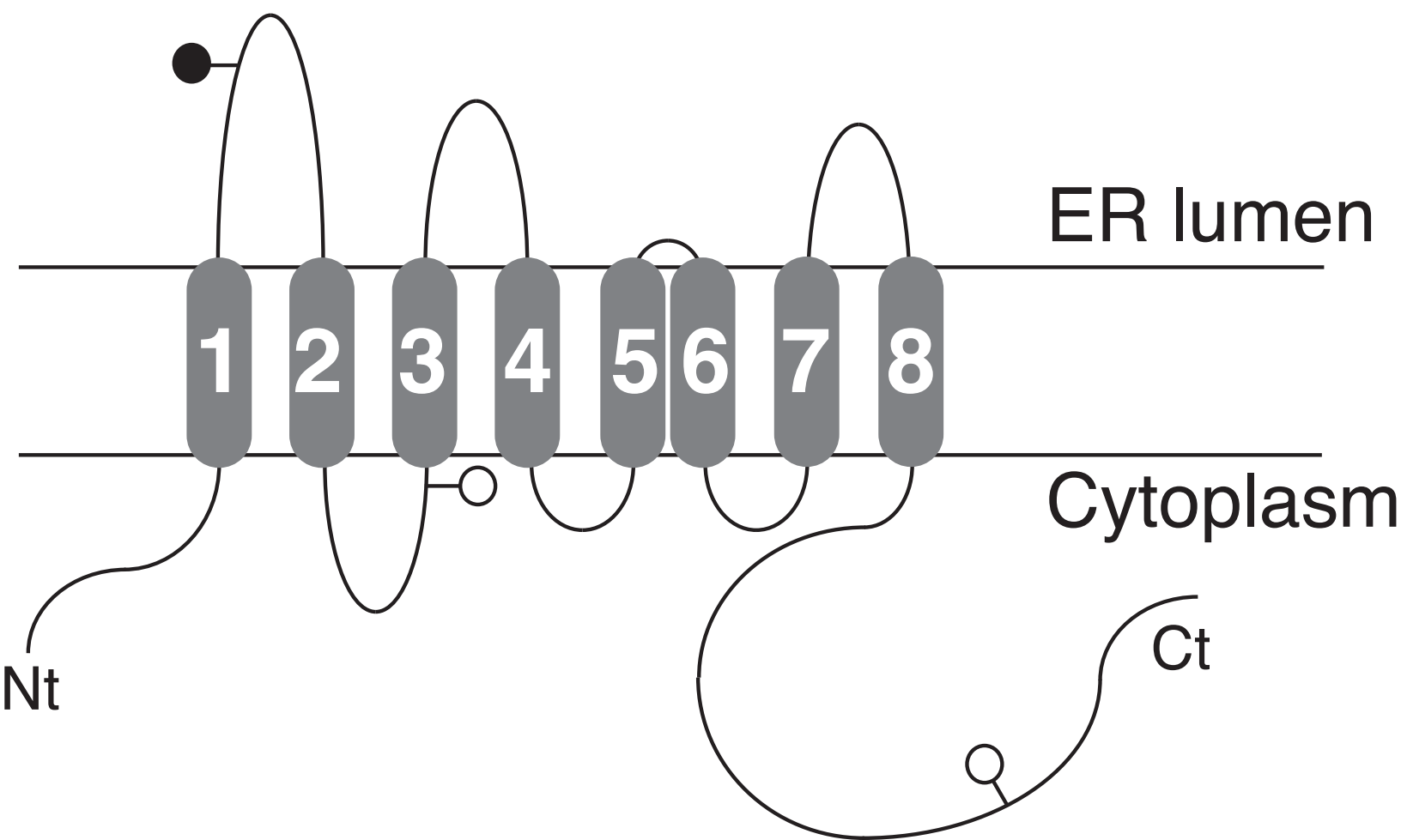
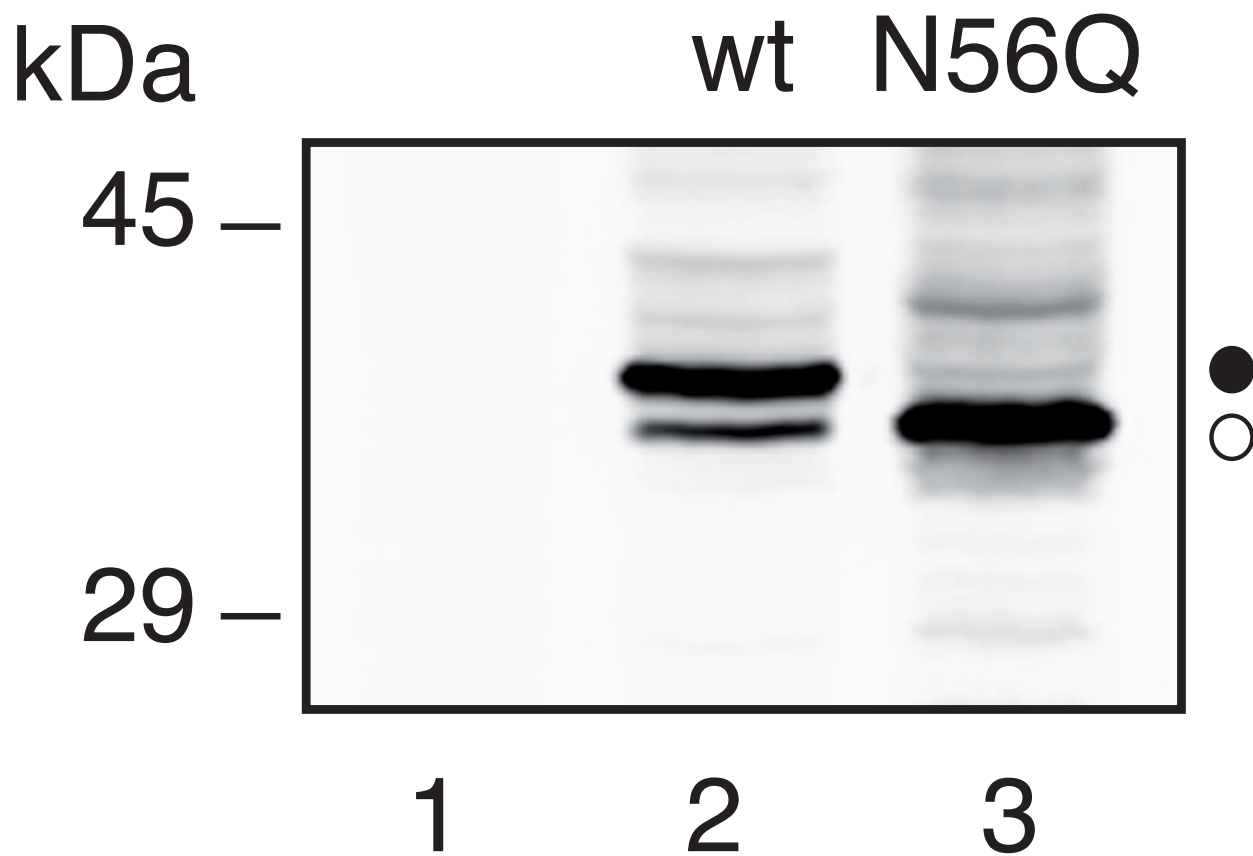
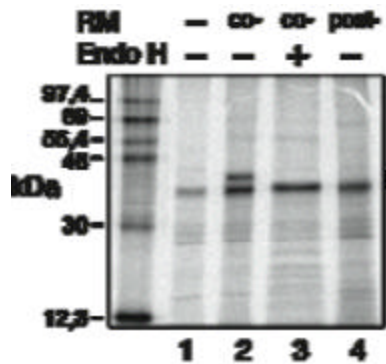


Figure 7



SUPPLEMENTARY FIGURES

Supplementary Fig. 1. *TRAM is inserted cotranslationally into the ER membrane.* TRAM was translated using reticulocyte lysates in either the absence (lanes 1 and 4) or the presence (lanes 2 and 3) of rough microsomes (RMs). In lane 3, the TRAM construct was translated in the presence of RMs and treated later with endoglycosidase H (Endo H), a glycan-removing enzyme. In lane 4, RMs were added posttranslationally (after 1 h and 10 min cycloheximide treatment) and incubation was continued for another 1 h. Non-glycosylated and glycosylated proteins are indicated by white and black dots, respectively.



Supplementary Fig. 2. *Insertion and topology of 119-mer and 129-mer truncates.* *In vitro* translation of mRNAs encoding nascent chains of 119-residues (119-mer, lanes 1-3) and 129-residues (129-mer, lanes 5-7) was achieved in the presence (+) or absence (-) of membranes and proteinase K (PK) as indicated. For the proteinase K protection assay, following translation the sample was supplemented with 1 μ L of 50 mM CaCl₂ and 1 μ L of proteinase K (2 mg/mL), then digested for 40 min on ice. The reaction was stopped by adding 2 mM PMSF before 20% SDS-PAGE analysis. Bands of non-glycosylated protein are indicated by a white dot and glycosylated proteins are indicated by a black dot. The brackets identify undigested polypeptides after PK treatment. It should be noted that proteinase K digestions are likely to occur at different positions at both N- and C-terminus of each polypeptide yielding the smear detected in lanes 3 and 7. Lane 4, ¹⁴C-labeled molecular weight markers.

